Physicochem. Probl. Miner. Process., 54(2), 2018, 578-589

http://www.journalssystem.com/ppmp/

Physicochemical Problems of Mineral Processing

ISSN 1643-1049

Received April 24, 2017; reviewed; accepted July 31, 2017

Activating flotation of chalcopyrite using $CuSO_4$ and H_2O_2 from the cyanide tailings

Guanghua Ai [1], Huashan Yan [2], Tingsheng Qiu [1], Cheng Liu [2]

[1] Faculty of Resource and Environmental Engineering, Jiangxi University of Science and Technology, Jiangxi 341000, China

[2] School of Mineral Processing and Bioengineering, Central South University, Changsha 410083, China

Corresponding author: guanghua_ai@126.com (Guanghua Ai)

Abstract: The effects of $CuSO_4$ and H_2O_2 on the flotation behavior of cyanide chalcopyrite were investigated by flotation tests, microcalorimetry and X-ray photoelectron spectroscopy (XPS). The underlying activation mechanism was studied in the perspective of micro-thermodynamics and surface properties. The flotation results indicated that cyanide chalcopyrite was strongly inhibited by sodium cyanide, with the maximum flotation recovery of 22.5% only. $CuSO_4$ and H_2O_2 significantly improved the flotation of cyanide chalcopyrite, and the flotation recovery was increased to 92.28% and 84.35%, respectively. The micro-thermodynamics results indicated that the adsorption heat of butyl xanthate on cyanide chalcopyrite surface increased after the addition of $CuSO_4$ and H_2O_2, as well as the reaction order. $CuSO_4$ and H_2O_2 can significantly improve the adsorption of butyl xanthate on the surface of cyanide chalcopyrite by decreasing the apparent activation energy by 80.11% and 66.54%, respectively. XPS analysis indicated that the CuCN was generated on the surface of cyanide chalcopyrite, leading to the loss of sulfur and inhibiting the adsorption of collectors. As a result, the flotation of cyanide chalcopyrite was depressed. It is considered that, $CuSO_4$ and H_2O_2 can improve the flotation of cyanide chalcopyrite by eleminating CuCN from its surface and increasing the concentration of S by 57.02% and 37.48%, respectively.

Keywords: *cyanide tailings, chalcopyrite, $CuSO_4$, H_2O_2, activation mechanism*

1. Introduction

Cyanide tailings are engendered from cyanidation gold extraction which has been rapidly developed since 1887 when the British chemist John Stewart MacArthur observed that cyanide could dissolve gold in the ore. This method gradually dominated in the gold extraction industry, such as high recovery, mature technology, low cost, etc. (Adams, 2005; Habashi, 1987), which resulted in the generation of tons of cyanide tailings. In statistics, more than 20 million tons cyanide tailings are discharged annually by Chinese gold mines (Li et al., 2011). And more cyanide tailings will be produced as the grade of recoverable gold-bearing ore is becoming lower and lower. Cyanide tailings were treated as waste in the early stage. With the substantial increase of the cyanide tailings, a large number of land resource is occupied and the environmental pollution becomes more and more serious, such as water pollution by the infiltration of residual flotation reagents in the tailings, air pollution caused by the solid dust particles, and the destruction of surrounding arable land quality (Laitos, 2013). In addition, the heavy metal ions in cyanide tailings, such as Cu^{2+}, Pb^{2+} and Zn^{2+}, as well as large amounts of undecomposed cyanide, pose a serious threat to the ecological environment and even the safety of human life (Donato et al., 2007; Mudder and Botz, 2004; Korte et al., 2000). At the same time, due to the limits of metallurgical technology, the cyanide tailings still contains lots of valuable elements, such as gold, silver, copper, lead, zinc, sulfur, iron and others. The grade of some elements are even higher than that of the raw ore, leading to a serious waste of resources if these

http://dx.doi.org/10.5277/ppmp1833

elements cannot be properly recovered. Therefore, it is of great significance to reduce the amount of cyanide tailings and recover the valuable elements.

Although the cyanide tailings contain a considerable amount of useful minerals (mostly sulfide minerals), the surface properties of these mineral particles have been totally different from those of the newly-exploited minerals due to their small particle size and prolonged contact with cyanide. As a result, they are hard to be recovered by froth flotation (Lv et al., 2016). The previous researchers (Guo et al., 2014; Zhao & Gu, 2013; Zhu & Zhu, 1996) proposed that the chemisorption of cyanide on the surface of sulfide minerals, and the dissolution of xanthate films on mineral surfaces made the mineral surfaces hydrophilic and difficult to float.

The recovery of valuable elements from cyanide tailings has been extensively reported in the literature (Liu, 2016; Xie et al., 2016; Yang et al., 2016). Li et al. (2009) tried to recover Cu and Pb from cyanide tailings by flotation of Pb and depression of Cu. They used lime to depress the flotation of pyrite and the residual cyanide to depress the flotation of chalcopyrite. And the combination reagents NP, the code name, was used as the activator of Cu, FM, the code name of reagent, as the inhibitor of pyrite, Z200 and ammonium dibutyl dithiophosphate as a composite collector of Cu. Finally, the Pb concentrate with a grade of 45.24% and Cu concentrate with a grade of 19.28% were achieved. Yang et al. (Yang et al., 2010) obtained a Pb concentrate with a grade of 49.93% from Shandong cyanide tailing, which contained a high grade of lead. A Zn concentrate with a grade of 48.86% was obtained from the tailing of Pb flotation, by using $CuSO_4$ as an activator, using H_2O_2 to remove the free CN^-, using CMC to depress Pb and gangue minerals. Lin et al. (Lin et al., 2013) used Na_2SO_3 and $ZnSO_4$ as the depressants of zinc-sulfur mineral, used PAC as the collector of Cu, and a Cu concentrate with a grade of 15.27% and a recovery of 80.55% was obtained. Zhang et al. (2011, 2013) carried out the recovery of iron in the cyanide slag. Yang et al. (2015, 2016) studied the recovery of copper sulfide ore from cyanide tailings by flotation, and found that the flotation of chalcopyrite and iron sphalerite were strongly depressed due to the chemisorption of CN^- on their surfaces, while sodium hypochlorite, H_2O_2, sodium meta-bisulfite and $CuSO_4$ could activate their flotation. However, the research on the recovery of valuable elements in cyanide tailings mainly focused on the process, while the underlying activation mechanism of the flotation of cyanide chalcopyrite remains unknown.

The flotation process is accompanied by a number of physical or chemical changes, such as the interaction and dissolution of reagents and mineral particles (Gao et al., 2017). The use of conventional means is often difficult to obtain useful information for a single reaction process, but with a more precise approach. Microcalorimetry is a method using microcalorimeters to continuously and accurately monitor micro energy changes in a reaction process and record their calorimetric curves, which is able to provide thermodynamic and kinetic information simultaneously in situ, in real time and losslessly (Chen and Bao, 2007a; Yang et al., 2014). At present, microcalorimetry has been widely used in chemical engineering, biochemistry, physical chemistry, organic chemistry and many other fields. However, the application of microcalorimetry in mineral processing is seldom reported. In the early years, Mellgren (1996) measured the adsorption heat of ethyl xanthate on galena. Haung and Miller (1978) examined the kinetics and thermochemistry of the xanthate adsorption reaction on pyrite and marcasite. The adsorption heats of 2-mercaptobenzoxazole (MBO) on chalcocite, 32-mercaptobenzothiazole (MBT) on galena and 2-aminothiophenol (ATP) on sphalerite were measured by Maier et al. (Maier et al., 1997). In recent years, microcalorimetric experiments were conducted to study dolomite, calcite and Icelandspar dissolution in HCl solutions by Chen et al. (Chen and Bao, 2007b; Chen et al., 2007), the results showed that reaction rates increase with decreases in mineral grain size and with increases in solution pH, and the relative mineral dissolution rates decrease from calcite, Iceland spar and dolomite. Wang et al. (2009) studied the influencing factors of the enthalpy variation during adsorption processes of acidithiobacillus ferrooxidans ATCC23270 on the surface of sulfide minerals and the metabolic thermogenesis of the bacteria under different conditions using microcalorimetry, and it was proved to be a good way to reflect the heat changes of bacterial growth patterns. Chen et al. (2013) investigated the adsorption of xanthate, dithiophosphate and dithiocarbamate on galena and pyrite surfaces by microcalorimetry, and concluded that the selectivity of dithiophosphate and dithiocarbamate were better than xanthate because of their greater difference in the adsorption heat and kinetics parameters. Zhao et al. (2014) studied the adsorption of water on

mineral surfaces using density functional theory and microcalorimetry technique. The calculation results showed that galena and molybdenite are hydrophobic, while pyrite and sphalerite is hydrophilic. Thermokinetic analysis showed that the heat of adsorption is in decreasing order of pyrite, sphalerite, galena and molybdenite, which is in good agreement with the calculation results, and the adsorption rate of water on the sphalerite surface is larger than that of water on the pyrite surface. Lan et al. evaluated the thermodynamic and kinetic parameters of adsorption of butyl xanthate on the surface of galena and six types of impurity-doped galena using microcalorimetry (Lan et al., 2016), and found that the adsorption heats of xanthate on the galena surface were directly proportional to the flotation recovery. Up to date, the application of microcalorimetry in the field of mineral processing is limited to the analysis of simple parameters, such as reaction heat, reaction order and reaction rate constant, without the further study of the activation energy. In addition, the mechanism study of the activating flotation using microcalorimetry is not reported.

In this work, the flotation behavior of cyanide chalcopyrite was studied using $CuSO_4$ and H_2O_2 as the activators through flotation test. Microcalorimetry was used for recording the calorimetric curves of the adsorption of BX on chalcopyrite samples at three temperatures, based on that, the related thermodynamic and kinetic parameters could be calculated to investigate the thermodynamic and kinetic law of chalcopyrite samples. X-ray photoelectron spectroscopy (XPS) tests was used for obtaining the surface composition and elements distribution of chalcopyrite samples. The activation mechanism and surface properties alteration of cyanide chalcopyrite were discussed indirectly and directly by microcalorimetry and XPS respectively.

2. Experimental

2.1 Materials and reagents

The single chalcopyrite mineral was obtained from a mine site in Jiangxi Province, China. The multi-element analysis shows that the purity of chalcopyrite is 98.58%. The XRD analysis is in consistent with the multi-element analysis. The particle size distribution of chalcopyrite is 44 um -74 um. The specific surface area of chalcopyrite measured by ASAP 2460 type Accelerated Surface Area and Porosimetry System (Micromeritics Instrument Co. Ltd., Shanghai, China) is 0.886 $m^2 \cdot g^{-1}$. The cyanide chalcopyrite samples were prepared in the laboratory by simulating the real cyanide leaching process. Chalcopyrite and 0.8% sodium cyanide solution were added to the sealed beaker at a solid / liquid ratio of 1: 9. The pH value was fixed at 12, and the rotational speed was 20 $r \cdot s^{-1}$ for 24 hours. The cyanide chalcopyrite was then obtained after filtering and drying in vacuum.

The chalcopyrite samples activated by $CuSO_4$ and H_2O_2 were prepared as follows: the cyanide chalcopyrite was placed in 40 cm^3 plexiglass tank of XFG-II flotation machine, and 0.2 mol $\cdot m^{-3}$ $CuSO_4$ solution and 1.8×10^3 $cm^3 \cdot m^{-3}$ H_2O_2 solution were added in order. The pH value was fixed at 10 and the conditioning lasted for 360 s at the speed of 30 $r \cdot s^{-1}$, followed by the filtering and drying in a vacuum oven. The amount of $CuSO_4$ and H_2O_2 were determined by flotation tests (Fig. 5).

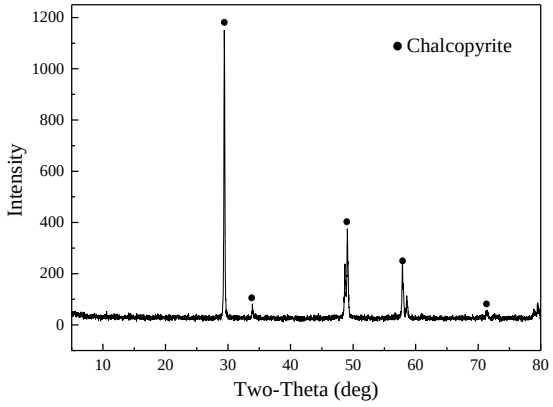

Fig. 1. XRD analysis of single chalcopyrite mineral

The butyl xanthate (BX) with purity greater than 95% was made in the laboratory. $CuSO_4$, H_2O_2 (30%), sodium hydroxide, and sodium cyanide, at an analytical grade, and 2# oil at an industrial grade were purchased from Sinopharm Chemical Reagent Company (Shanghai, China).

2.2 Flotation tests

The flotation test was carried out in a 40 cm^3 XFG-II flotation machine (China Prospecting Machinery Factory, China), as shown in previous publications (Gao et al., 2016a, b). For each test, 2.0 g mineral samples and 20 cm^3 of distilled water were put into the beaker. The mixture was vibrated ultrasonically for 5 min by ultrasonic cleaner, then allowed to stand for a few minutes until the liquid was divided into two layers. The mineral samples was for flotation tests after sucking the supernatant. The distilled water, pH adjusting agent, activator, collector and frother were added in turn, and the condition time after each addition was 60 s, 120 s, 180 s, 180 s and 120 s, respectively. The artificial scraping time was 240 s. The flotation process was shown in Fig. 2. The foam concentrates and tailings were filtered, dried and weighed to calculate the mass recovery. Each flotation test were repeated three times, the average reported as the final value.

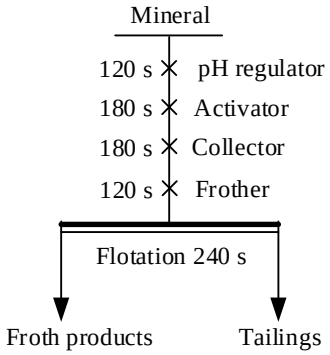

Fig. 2. The schematic of flotation test

2.3 Microcalorimetry analysis

The calorimetric measurements at 298.15 K, 301.15 K and 304.15 K were carried out using the RD496-2000 microcalorimeter, and the calorimetric constants of the microcalorimeter at these three temperatures were 6.667×10^{-2} V·W^{-1}, 6.638×10^{-2} V·W^{-1} and 6.627×10^{-2} V·W^{-1}, respectively, measured by Joule effect experiment. The measurement part of the microcalorimeter consists of two identical thermopiles (P1 and P2) (Fig. 3 (a) -1).

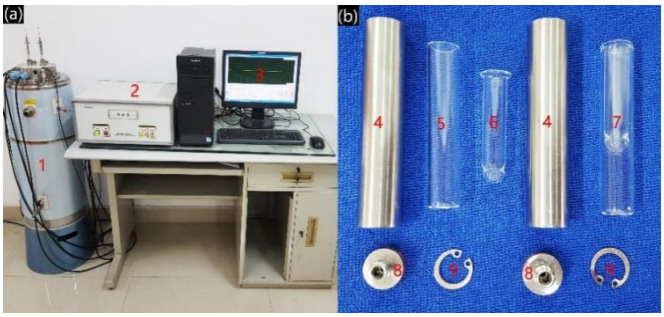

Fig. 3. The photo of RD496-2000 microcalorimeter and test tools. 1-calorimeter; 2-CK-2000 monitoring and control; 3-computer; 4-stainless steel pipe; 5-glass outer tube; 6-glass inner tube; 7-glass sleeve (inner tube + outer tube); 8-perforated upper end cap; 9-hole elastic snap ring

P1 is placed in the "measurement cell" and P2 is in the reference cell. The difference between the two thermopiles (P1-P2) is the thermal effect of the adsorption process. For each measurement, 0.03 g of sample and 1 cm^3 of distilled water were placed in a glass outer tube (Fig. 3 (b) -5). And collector

solution was added to a glass inner tube (Fig. 3 (b) -6). The glass inner tubes were placed in a glass outer tube (Fig. 3 (b) -7), which were then placed in a stainless steel tube (Fig. 3 (b) -4) B) -8). And the "measurement cell" was ready after fastening the hole with a snap ring (Fig. 3 (b) -9). The "reference sample cell" was the same as the "measurement cell" except that no mineral sample was added to the glass outer tube. Through this way, the dilution enthalpy of butyl xanthate solution can be eliminated during the calorimetric test, and more accurate thermo-kinetic data can be obtained. The "measurement cell" and the "reference cell" were put into the thermopile P1 and P2, respectively, and the temperature was fixed at 293.15 K. When the baseline was stabilized, the glass needle was pushed down rapidly and the inner glass tube in the two sample cells was pierced. The BX solution in the "measurement cell" was mixed with the mineral sample solution, and the BX solution in the "reference sample cell" was mixed with the distilled water. The thermal difference between the two thermopiles (P1-P2) recorded by the computer was the adsorption heat of BX on the mineral surface. And its calorimetric curve was presented on the computer simultaneously.

2.4 XPS analysis

The XPS analysis was carried out using an ESCALAB 250 photoelectron spectrometer (Thermo Fisher Scientific Co., USA) with an X-ray source of the monochromatic Al-Kα source operating at 1.2×10^4 V and an analysis chamber vacuum 2×10^{-7} Pa (open X-ray source in the case). The instrumental error is ± 0.2 eV (1 eV = 1.6×10^{-19} J). The preparation method of the test sample was as follows: 0.5 g mineral samples were placed in test tubes, followed by the addition of distilled water and 300 s ultrasonic cleaning. The sample was dried in 313.15 K vacuum oven after filtration.

3. Results and discussion

3.1 Flotation behavior of chalcopyrite

To study the flotation behavior of cyanide chalcopyrite before and after activation and to determine the concentration of BX solution used in the following calorimetric test, the effects of BX, as well as the $CuSO_4$ and H_2O_2, on the flotation behavior of the cyanide chalcopyrite were investigated in details.

3.1.1 Effect of BX on the flotation of cyanide chalcopyrite

Fig. 4 shows the flotation results of cyanide chalcopyrite using BX as collectors. The recovery increased gradually with an increase in BX dosage, and reached the maximum of about 22.5% when the dosage of BX reached 0.08~0.1 mol·m^{-3}. After that, the chalcopyrite recovery did not increase with the further addition of BX. The results indicated that chalcopyrite was significantly depressed by sodium cyanide, and it is difficult to achieve a high recovery by increasing BX dosage only. It is considered that, the adsorption of BX on chalcopyrite surface increased with an increase in its dosage, and started to saturate when its dosage was 0.08~0.1 mol·m^{-3}. As a result, the recovery could hardly increase with the further addition of BX. Based on the above analysis, the concentration of BX solution used in the calorimetric test was determined to be 0.1 mol·m^{-3}.

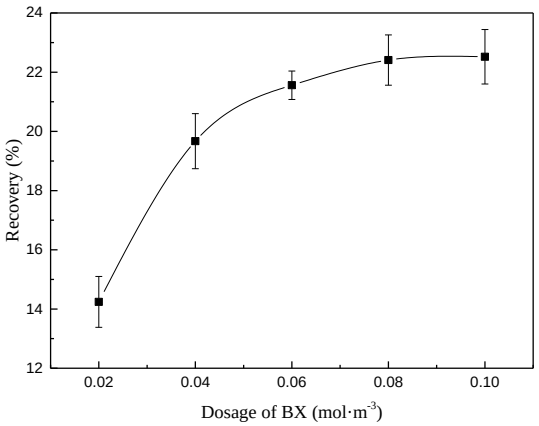

Fig. 4. Effect of BX on flotation recovery of cyanide chalcopyrite

3.1.2 Effect of $CuSO_4$ and H_2O_2 on the recovery of cyanide chalcopyrite

Fig. 5 gives the flotation results of cyanide chalcopyrite after the addition of $CuSO_4$ and H_2O_2. The recovery of chalcopyrite increased significantly with an increase in the $CuSO_4$ dosage, and close to the maximum of 92.28% when $CuSO_4$ dosage reached 0.2 mol·m^{-3}. After that, the recovery of chalcopyrite remained stable with the further addition of $CuSO_4$. This is because Cu^{2+} can slightly oxidize CN^- into $(CN)_2$ or directly interact with CN^- and give rise to copper cyanide complex precipitation, the CN^- on the surface of chalcopyrite was consumed. Through this way, cyanide chalcopyrite can be activated by $CuSO_4$.

Compared with $CuSO_4$, H_2O_2 is a strong oxidant and it can preferentially oxidize CN^-. As shown in Fig. 5, the recovery of chalcopyrite increased rapidly with an increase in the H_2O_2 dosage, and peaked at 84.35% when H_2O_2 dosage was 1.8×10^3 cm^3·m^{-3}. It is considered that the CN^- on the surface of cyanide chalcopyrite was consumed by H_2O_2 and the fresh chalcopyrite surface was generated. And the maximum flotation recovery was achieved when all the CN^- was consumed. After that, with the further addition of H_2O_2, the low-valent S was oxidized to high-valence sulfur, leading to the decrease of chalcopyrite hydrophobicity. As a result, the recovery decreased drastically.

Above all, both $CuSO_4$ and H_2O_2 have good activation effects for the flotation of cyanide chalcopyrite, and $CuSO_4$ was better than H_2O_2.

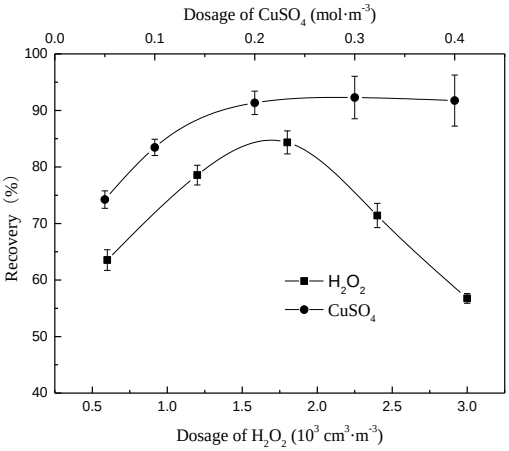

Fig. 5. Effect of $CuSO_4$ and H_2O_2 on the flotation recovery of cyanide chalcopyrite

3.2 Micro-thermodynamics study

The key to the flotation process is the interactions between collectors and target minerals. In this work, the adsorption of collectors on the surface of chalcopyrite was monitored and recorded using microthermometer which is sensitive to thermal effect, so as to study the role of $CuSO_4$ and H_2O_2 in the flotation of cyanide chalcopyrite in terms of micro-thermodynamics.

3.2.1 The calorimetry curve of the adsorption of BX on chalcopyrite surface

The calorimetry curves of the adsorption of BX on different chalcopyrite surfaces were recorded using a microcalorimeter (Fig. 6). In Fig. 6, the horizontal axis is the adsorption time and the vertical axis is the heat flow which represents the instantaneous adsorption heat. The total calorific value can be obtained through the calculation of the area formed by the calorimetric curve and the t-axis, which is also the adsorption heat, Q. In addition, the process is exothermic if the calorimetric curve is positive, otherwise, the process is endothermic.

All the calorimetry curves in Fig. 6 are positive, indicating that the adsorption of BX was exothermic. The calorimeter curve of BX adsorption moved to left with an increase in the temperature, suggesting that the reaction rate increased with temperature while the adsorption heat decreased simultaneously, which is in consistent with the thermochemical laws of exothermic reactions. Furthermore, the adsorption heat of BX on chalcopyrite surface increased significantly after the

addition of two activators, indicating that the two activators substantially eliminated CN^- from the chalcopyrite surface and generated the fresh surface again.

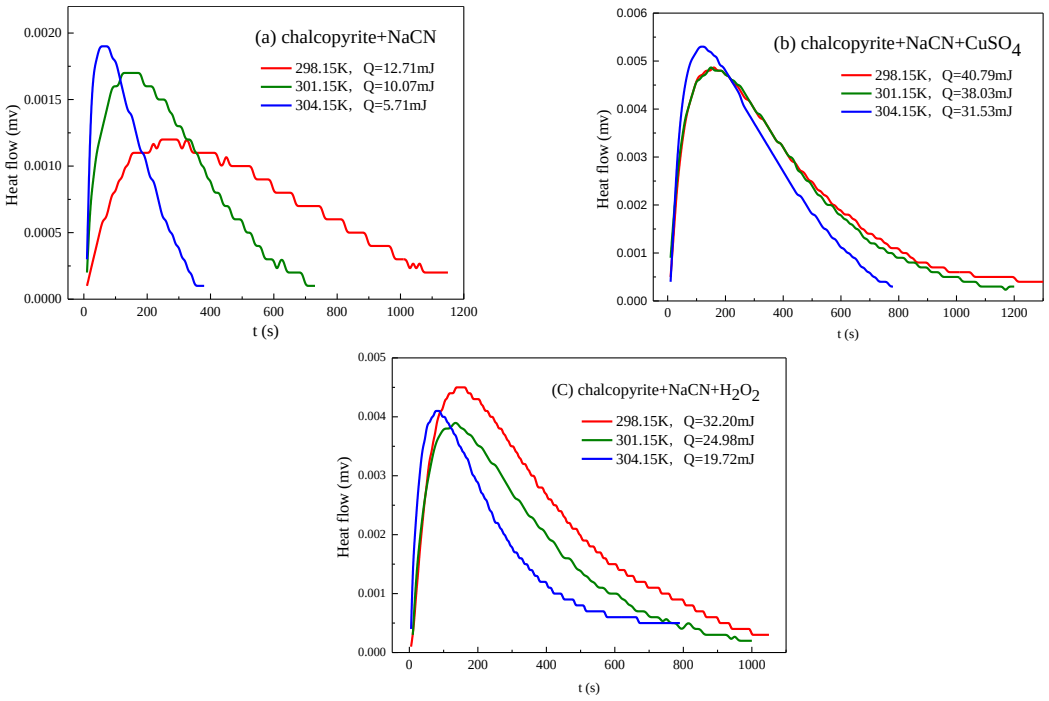

Fig.6. Calorimetric curve of the adsorption of BX on chalcopyrite surface

3.2.2 Kinetics and thermodynamic parameters

The calorimetric curve in Fig. 6 was processed using the method described by Gao et al. (Gao et al., 2002; Zhao et al., 2014). The relation of enthalpy change and reaction rate is shown by micro-thermodynamics formula of Eq. (1):

$$\ln\left(\frac{1}{H_0}\cdot\frac{\mathrm{d}H_i}{\mathrm{d}t}\right)=\ln k+n\ln\left(1-\frac{H_i}{H_0}\right), \tag{1}$$

where n is reaction order and H_0 is the total enthalpy of system. The lnk in the plot of $\ln\left(\frac{1}{H_0}\cdot\frac{\mathrm{d}H_i}{\mathrm{d}t}\right)$ against $\ln\left(1-\frac{H_i}{H_0}\right)$ is determined from the intercept of $\ln\left(\frac{1}{H_0}\cdot\frac{\mathrm{d}H_i}{\mathrm{d}t}\right)$ with y-axis, by which the rate constant (k) of the reaction is calculated. The slope of curve is the reaction order (n). On the basis of the rate constant (k) at each temperature, the apparent activation energy (E_a) and the pre-exponential factor (lnA) can be calculated by the same method according to Eq. (2):

$$\ln k=\ln A-\left(\frac{E_a}{RT}\right), \tag{2}$$

where R is molar gas constant and T is temperature. The results of relevant kinetics and thermodynamics parameters are summarized in Table 1.

In Table 1, Q_u is the adsorption heat per unit area, which is calculated by the samples quality, specific surface area, and total adsorption heat.

Table 1 indicates that, with an increase in the temperature, the adsorption heat per unit area decreased while the reaction rate increased simultaneously, which is in consistent with the law of the calorimetric curve. Compared with cyanide chalcopyrite, the adsorption heat per unit area of BX on the surface of chalcopyrite increased significantly after conditioning with the two activators. At the same time, the corresponding reaction order also increased to some extents. This suggested that $CuSO_4$ and H_2O_2 had caused significant changes to the surface of cyanide chalcopyrite.

The difficulty of a reaction can be directly reflected by the apparent activation energy. A significant difference of the apparent activation energy for the adsorption of BX on the surface of different chalcopyrite can be observed from Table 1. The apparent activation energy of the adsorption of BX on

the surface of cyanide chalcopyrite, H_2O_2 activated chalcopyrite, and $CuSO_4$ activated chalcopyrite was 164.96 KJ·mol^{-1}, 55.19 KJ·mol^{-1} and 32.81 KJ·mol^{-1}, respectively. This means that the difficulty of the adsorption of BX on the surface of these three types of chalcopyrite decreased in turn, which was in consistent with their corresponding flotation recovery. The results indicate that $CuSO_4$ and H_2O_2 can significantly reduce the apparent activation energy of the adsorption of BX on the surface of cyanide chalcopyrite, decreased by 80.11% and 66.54%, respectively, so as to achieve an efficient flotation recovery of chalcopyrite.

Table 1. The kinetics and thermodynamic parameters of the adsorption of BX on chalcopyrite surface

Adsorption conditions	T/ K	Q_u/ J·m^2	K/10^{-3} s^{-1}	n	lnA /s^{-1}	E_a/ kJ·mol^{-1}
chalcopyrite+NaCN	298.15	0.478	1.71	0.46	60.17	164.96
	301.15	0.379	3.31	0.55		
	304.15	0.215	6.34	0.58		
chalcopyrite+NaCN+$CuSO_4$	298.15	1.535	2.46	0.86	7.21	32.81
	301.15	1.431	2.63	0.76		
	304.15	1.186	3.20	0.63		
chalcopyrite+NaCN+H_2O_2	298.15	1.211	2.79	0.78	16.35	55.19
	301.15	0.940	3.17	0.79		
	304.15	0.742	4.34	1.00		

3.3 XPS analysis

The XPS analysis (Jia et al., 2000; Decines et al., 2003; Liu et al., 2010) of three types of chalcopyrite was carried out, and the XPS spectrum of chalcopyrite surface, the spectrum of Cu 2p and the concentration of elements are shown in Fig. 7, Fig. 8 and Table 2, respectively. Peaks fitting of XPS spectrum were conducted by XPSPEAK software.

3.3.1 XPS spectrum of chalcopyrite surface

Fig. 7 shows the XPS spectrum of chalcopyrite surface. The spectrum of three types of chalcopyrite was fitted to different elements according to their binding energies. The peak at the binding energy of 160 eV, 710 eV, and 930 eV corresponded to S 2p, Fe 2p, and Cu 2p, respectively. In addition, there were also peaks occurring at 285 eV and 530 eV, which are the binding energies of C 1s and O 1s. This can be attributed to the carbon and oxygen contamination. In addition, all the XPS spectra of the three chalcopyrite surfaces show characteristic peaks of N 1s at the binding energy of about 400 eV. Compared to the cyanide chalcopyrite, the intensities of N 1s peaks on the surface of chalcopyrite activated by two activators were significantly weakened. The results indicate that the two activators can destroy and release the chemically adsorbed CN^- on the surface of cyanide chalcopyrite, so as to activate the flotation of chalcopyrite.

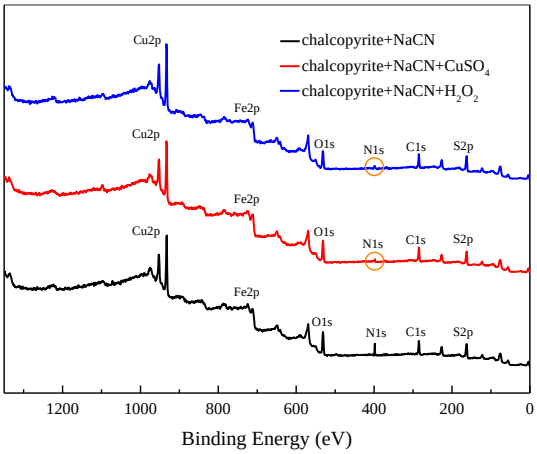

Fig. 7. XPS spectrum of chalcopyrite surface

3.3.2 XPS spectrum of Cu 2p

Fig. 8 gives the XPS spectrum of Cu 2p. The peak of Cu 2p was fitted to three peaks at the binding energy of 931.8 eV, 932.5 eV, and 933.1 eV, representing the contributions of Cu from $CuFeS_2$, CuS, and CuCN. Fig. 8 (a) indicates that the main types of Cu on the surface of cyanide chalcopyrite are $CuFeS_2$ and CuCN. The peak area of CuCN was almost same as that of $CuFeS_2$ with only a small amount of CuS, indicating that CuCN was the major product of the chemisorption of CN^- on chalcopyrite surface. Fig. 8 (b) and (c) show that the main types of Cu on the surface of chalcopyrite activated by $CuSO_4$ and H_2O_2 were $CuFeS_2$, followed by CuCN. Compared to chalcopyrite without activation, the content of CuCN on the surface of chalcopyrite decreased significantly after interacting with two activators. In addition, there was also a small amount of CuS on the surface of two types of chalcopyrite with least peak area.

It can be known from Fig. 8 (a), (b) and (c) that the peak area of CuCN on three types of chalcopyrite was in the following order: cyanide chalcopyrite > H_2O_2 activated chalcopyrite > $CuSO_4$ activated chalcopyrite. This is also in accordance with the flotation recovery.

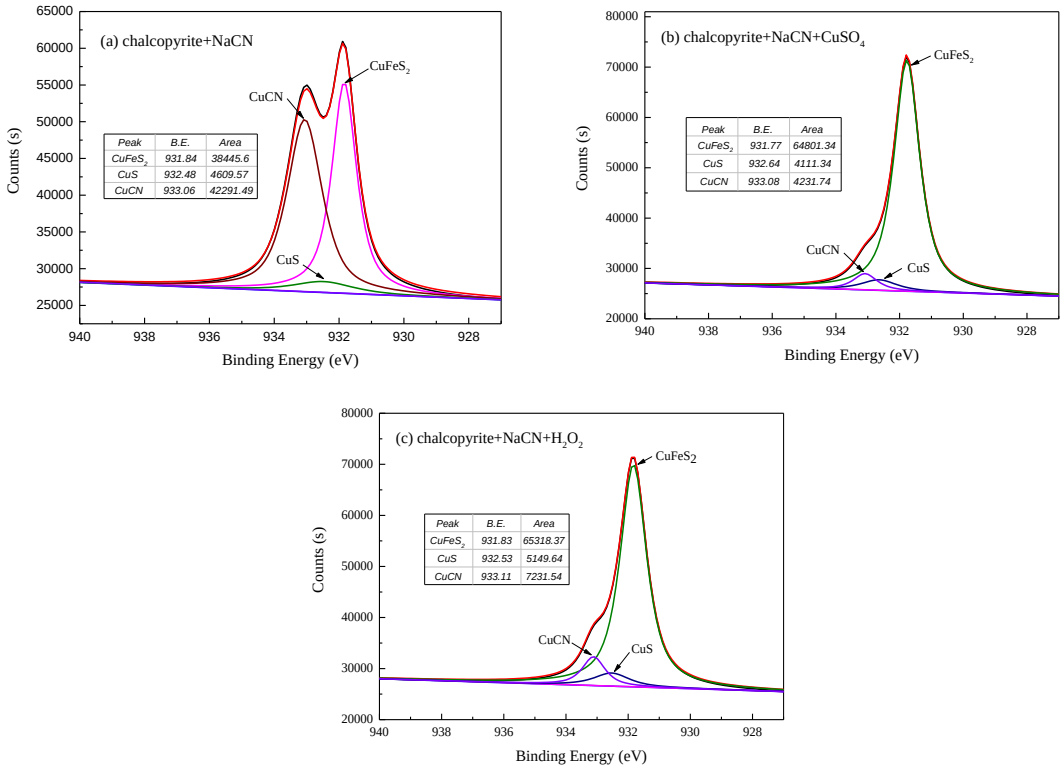

Fig. 8. XPS spectrum of Cu 2p on the surface of chalcopyrite before and after activation

3.3.3 Elements concentration on the surface of chalcopyrite

Table 2 demonstrates that due to the presence of CuCN, the concentration of S element on the surface of cyanide chalcopyrite was only 18.73%, while the concentration of N element was as high as 7.63%. After activation by $CuSO_4$ and H_2O_2, the concentration of S on the surface of chalcopyrite increased by 57.02% and 37.48%, respectively, while the concentration of N decreased dramatically to 0.62% and 0.98%.

In addition, the element concentration ratio on the surface of pure chalcopyrite should be Cu: Fe: S = 1: 1: 2, while the ratio on the surface of cyanide chalcopyrite was Cu: Fe: S=1: 0.6: 1.07. There is a significant sulfur loss on the surface of cyanide chalcopyrite, which is not good for the adsorption of the collector. After activation by $CuSO_4$ and H_2O_2, the element concentration ratio on the surface of chalcopyrite (Cu: Fe: S) became 1: 0.95: 1.93 and 1: 0.84: 1.74, which are close to that of pure chalcopyrite. The results indicated that the concentration of S on chalcopyrite surface has been significantly enhanced.

Above all, both activators can effectively remove CN^- from the surface of chalcopyrite and reduce the concentration of N. They can greatly increase the concentration of S on the surface of chalcopyrite, and the effect of $CuSO_4$ is slightly better than that of H_2O_2.

Table 2. The elements concentration on the surface of chalcopyrite

Sample	Elements concentration / %				Elements concentration ratio (Cu: Fe: S)
	Cu	Fe	S	N	
Chalcopyrite +NaCN	17.45	10.39	18.73	7.63	1:0.6:1.07
Chalcopyrite +NaCN+$CuSO_4$	15.26	14.57	29.41	0.62	1:0.95:1.93
Chalcopyrite +NaCN+H_2O_2	14.83	12.47	25.75	0.98	1:0.84:1.74

4. Conclusions

(1) The flotation results indicated that cyanide chalcopyrite was strongly inhibited, with the maximum flotation recovery of 22.5%, and $CuSO_4$ and H_2O_2 showed the good activating effect on it. The flotation recovery of cyanide chalcopyrite after activation by $CuSO_4$ and H_2O_2 increased to 92.28% and 84.35%, respectively.

(2) The micro- thermokinetics results showed that the adsorptions of BX on chalcopyrite surfaces were exothermic, the heats and reaction orders of BX adsorption on the surface of cyanide chalcopyrite increased with the addition of $CuSO_4$ and H_2O_2. $CuSO_4$ and H_2O_2 can significantly reduce the apparent activation energy of the adsorption of BX on the surface of cyanide chalcopyrite, decreased by 80.11% and 66.54%, respectively, which can improve the adsorption of BX.

(3) XPS analysis revealed that lots of CuCN presented on the surface of cyanide chalcopyrite, which led to the loss of sulfur and inhibited the adsorption of collectors. As a result, the flotation of cyanide chalcopyrite was depressed. $CuSO_4$ and H_2O_2 could effectively eliminate CuCN from the surface of cyanide chalcopyrite, and the concentration of S increased by 57.02% and 37.48%, respectively, which greatly improved the sulfur loss state on the surface of cyanide chalcopyrite, and the element concentration ratio (Cu: Fe: S) from 1: 0.6: 1.07 became to 1: 0.95: 1.93 and 1: 0.84: 1.74. Therefore, $CuSO_4$ and H_2O_2 can activate the flotation of chalcopyrite in the cyanide tailings which is strongly inhibited by sodium cyanide.

Acknowledgements

This work was financially supported by the Projects of National Natural Science Foundation of China (No. 51474114 and No. 51564014). This work was also supported by the Program for Excellent Young Talents, JXUST, China.

References

ADAMS, M. D., 2005. *Advances in Gold Ore Processing*. Elsevier Ltd., Chapter 20.

CHEN, J. H., LAN, L. H., CHEN, Y., 2013. *Computational simulation of adsorption and thermodynamic study of xanthate, dithiophosphate and dithiocarbamate on galena and pyrite surfaces*. Mineral Engineering, 46-47, 136-143.

CHEN, J. W., BAO, Z. Y., 2007a. *Advances in the calorimetry and the thermokinetic study*. Geological Bulletin of China, 12, 1564-1568 (in Chinese).

CHEN, J. W., BAO, Z. Y., 2007b. *Thermo-kinetic study on mineral dissolution by microcalorimetry*. in: The Twelfth International Symposium on Water-Rock Interaction 1, 289-291.

CHEN, J. W., BAO, Z. Y., MEI, Y. P., 2007. *Experimental study on mineral dissolution reaction by microcalorimetry*. Bulletin of Mineralogy, Petrology and Geochemistry Sup 1, 496-497 (in Chinese).

DECINES, D., LI, C. G., CUI H. S., 2003. *Interaction of gold and sulfide minerals in a cyanide medium*. Metallic Ore Dressing Abroad 8, 32-39 (in Chinese).

DONATO, D., NICHOLS, O., POSSINGHAM, H., MOORE, M., RICCI, P., NOLLER, B., 2007. *A critical review of the effects of gold cyanide-bearing tailings solutions on wildlife*. Environ. Int., 7, 974-984.

GAO, S. L., CHEN, S. P., HU, R. Z., et al., 2002. *Derivation and application of thermodynamic equations*. Chinese Journal of Inorganic Chemistry, 4, 362-366 (in Chinese).

GAO, Y.S., GAO, Z.Y., SUN, W., HU, Y.H., 2016 a. *Selective flotation of scheelite from calcite: A novel reagent scheme*. International Journal of Mineral Processing, 154, 10-15.

GAO, Z.Y., GAO, Y.S., ZHU, Y.Y., HU, Y.H., SUN, W., 2016 b. *Selective flotation of calcite from fluorite: a novel reagent schedule*. Minerals, 6(4), 114.

GAO, Z., LI, C., SUN, W., HU, Y., 2017. *Anisotropic surface properties of calcite: A consideration of surface broken bonds*. Colloid. Surface. A., 520, 53-61.

GUO, B., PENG, Y. J. RODOLFO, E. G., 2014. *Cyanide chemistry and its effect on mineral flotation*. Minerals Engineering, 66-68, 25-32.

HABASHI, F., 1987. *One hundred years of cyanidation*. Mining and Metallergical Bulletin, 905,108-114.

HAUNG, H. H., MILLER, J. D., 1978. *Kinetics and thermochemistry of amyl xanthate adsorption by pyrite and marcasite*. International Journal of Mineral Processing, 5, 241-266.

JIA, J. Y., XIE, X. D., WU, D. Q., WANG, J. C., WANG, Y., 2000. *An XPS Study on Surfaces of Common Sulfide Minerals*. Geological Journal of China Universities, 2, 255-259 (in Chinese).

KORTE, F., SPITELLER, M., COULSTON, F., 2000. *The cyanide leaching gold recovery process is a nonsustainable technology with unacceptable impacts on ecosystems and humans: the disaster in Romania*. Ecotoxicol. Environ. Saf., 3, 241-245.

LAITOS, J. G., 2013. *Cyanide, mining, and the environment*. Pace Environmental Law Review, 3, 869-1278.

LAN, L. H., CHEN, J. H., LI, Y. Q., et al., 2016. *Microthermokinetic study of xanthate adsorption on impurity-doped galena*. Transactions of Nonferrous Metals Society of China, 1, 1-25.

LI, T., YIN, Y. F., FANG, X. H., et al., 2011. *Technological status of recovering copper, lead, zinc, sulfur from gold cyaniding tailings*. Modern Mining, 4, 28-29 (in Chinese).

LI, Z. Y., WANG, L., YU, H. Y., et al., 2009. *Recovery of lead and copper from cyanide tailings*. Journal of University of Science and Technology Beijing, 10, 1231-1234 (in Chinese).

LIN, J. L., LI, Z. H., LU, Y. W., et al., 2013. *Research on recoverying copper from cyanide tailing of a gold ore in Xinjiang*. Multipurpose Utilization of Mineral Resources, 2, 28-32 (in Chinese).

LIU, C. L., 2016. *Comprehensive polymetallic recovery from silver cyanide slag*. Nonferrous Metals (mineral processing section), 3, 38-42 (in Chinese).

LIU, S. J., HE, F. Y., SONG L., 2010. *Effect of grinding mode on surface property and flotation behavior of chalcopyrite*. Nonferrous Metals (Mineral Processing Section), 6, 35-40 (in Chinese).

LIU, X. W., CHEN, J. W., BAO, Z. Y., et al., 2002. *Relationship between the thermal kinetics of dissolution and crystal defects of several minerals*. Journal of Chinese Electron Microscopy Society, 5, 751-752 (in Chinese).

LV, C. C., DING, J., FU, G. Y., et al., 2016. *Present situation and prospect of recovering valuable elements from cyanidation tailing*. CIESC Journal, 4, 1079-1089 (in Chinese).

MAIER, G. S., QIU, X., DOBIAS, B., 1997. *New collectors in the flotation of sulphide minerals: a study of the electrokinetic, calorimetric and flotation properties of sphalerite, galena and chalcocite*. Physicochemical and Engineering Aspects, 122, 207-225.

MELLGREN, O., 1966. *Heat of adsorption and surface reactions of potassium ethyl xanthate on galena*. Transactions Society of Mining Engineers, 235, 46-59.

MUDDER, T., BOTZ, M., 2004. *Cyanide and society: a critical review*. European Journal of Mineral Processing and Environmental Protection, 1, 62-74.

WANG, X. M., LIU, J. S., LI, B. M., et al., 2009. *Study on the Enthalpy Variation during Adsorption Processes of Acidithiobacillus ferrooxidans ATCC23270 on the Surface of Minerals and Its Metabolic Thermogenesis under Different Conditions*. Geological Journal of China Universities, 15, 256-262 (in Chinese).

XIE, K., ZOU, S., CHEN, J., PENG, J., 2016. *Experimental study on recovering gold from cyanidation tailings and biosafety disposal*. GOLD, 37, 58-61 (in Chinese).

YANG, J. Y., CHEN, P., XU, X. B., LI, X. L., FAN, L. W., XU, Z. M., 2016. *Experimental research on comprehensive recovery of copper, lead and zinc from low grade cyanide tailings in Jiaodong region*. GOLD, 2, 68-71 (in Chinese).

YANG, Q., CHEN, S. P., XIE, G., et al., 2014. *Development and application of RD496 microcalorimeter*. Scientia Sinica Chimica, 6, 889-914 (in Chinese).

YANG, W., QIN, W. Q., LIU, R. Q., 2010. *Study on the separation of lead and zinc in cyaniding tailings*. Mining and Metallurgical Engineering 6, 30-33 (in Chinese).

YANG, X. L., HUANG, X., QIU, T. S., 2015. *Recovery of zinc from cyanide tailings by flotation*. Minerals Engineering, 84, 100-105.

YANG, X. L., HUANG, X., QIU, T. S., 2016. *Activation of sodium metabisulfite on surfaces of copper-zinc sulfide ore in cyanidation tailings*. The Chinese Journal of Nonferrous Metals, 9, 1982-1989 (in Chinese).

ZHANG, Y. L., LI, H. M., YU, X. J., 2013. *Fe extraction from high-silicon and aluminum cyanide tailings by magnetic separation pretreatment of water leaching before magnetic separation*. Transactions of Nonferrous Metals Society of China, 4, 1165-1173.

ZHANG, Y. L., YU, X. J., LI, X. B., ZHANG, L. P., LI, D. G., 2011. *Thermodynamics analysis of ferric compound during roasting-preparing process of cyanide tailings*. Journal of Central South University (Science and Technology), 12, 3623-3629 (in Chinese).

ZHAO, C. H., CHEN, J. H., LONG, X. H., GUO, J., 2014. *Study of H_2O adsorption on sulfides surfaces and thermokinetic analysis*. Journal of Industrial and Engineering Chemistry, 20, 605-609.

ZHAO, H. D., GU, G. H., 2013. *Status and Prospect of Research on Comprehensive Recovering Copper, Lead and Zinc from Cyaniding Residues*. Multipurpose Utilization of Mineral Resources, 5, 1-4 (in Chinese).

ZHU, Y. S., ZHU, J. G., 1996. *Chemical Principles of Flotation Agent*. Central South University Press, Changsha, Chap. 2.